

Rapid deposition of YBCO films by laser CVD and effect of lattice mismatch on their epitaxial growth and critical temperature

Pei Zhao, Akihiko Ito*, Takashi Goto

Institute for Materials Research, Tohoku University, 2-1-1 Katahira, Aoba-ku, Sendai 980-8577, Japan

Received 15 January 2013; received in revised form 26 February 2013; accepted 28 February 2013

Available online 14 March 2013

Abstract

a-Axis- and *c*-axis-oriented $\text{YBa}_2\text{Cu}_3\text{O}_{7-\delta}$ (YBCO) films were grown on (100) SrTiO_3 substrate by laser chemical vapour deposition (laser CVD). The effect of lattice mismatch between films and substrates on in-plane and out-of-plane crystallinity and critical temperature (T_C) was investigated. The preferred orientation changed from *a*-axis to *c*-axis as the deposition temperature increased from 928 to 1049 K. The *c*-axis-oriented YBCO showed a minimum of full width at half maximum of 0.5° for the ω -scan and 1.0° for the ϕ -scan. A smaller mismatch between YBCO films and substrates led a higher crystallinity for in-plane and out-of-plane epitaxial growths. A high T_C of 90 K was obtained for the *c*-axis-oriented YBCO films. The deposition rate of the YBCO films was $58\text{--}101\text{ }\mu\text{m h}^{-1}$, approximately 60–1000 times higher than that of conventional CVD.

© 2013 Elsevier Ltd and Techna Group S.r.l. All rights reserved.

Keywords: $\text{YBa}_2\text{Cu}_3\text{O}_{7-\delta}$; Laser chemical vapour deposition; Epitaxial growth; Critical temperature

1. Introduction

Among the various thin-film preparing techniques, metalorganic chemical vapour deposition (MOCVD) for the preparation of $\text{YBa}_2\text{Cu}_3\text{O}_{7-\delta}$ (YBCO) films is promising because it offers uniform coverage, excellent control of composition and can coat large areas of substrates with complex shape. MOCVD YBCO films exhibit high current density of $10^5\text{--}10^6\text{ A cm}^{-2}$ at the boiling point of liquid N_2 (77 K) [1–3], indicating great potential in industrial applications. MOCVD is cost effective and suitable for scaling up to continuous preparation by using a reel-to-reel system [4–7]. However, the drawback of MOCVD is the low deposition rate of 0.01 to several micrometer per hour.

In contrast, laser-assisted chemical vapour deposition (laser CVD) can grow various oxide films, such as Al_2O_3 [8], Ba_2TiO_5 [9], at significantly high deposition rates (several tens to hundreds micrometer per hour). We have epitaxially grown YBCO films on (100) MgO [10] and (100) LaAlO_3 (LAO) [11] single-crystal substrates by using laser CVD at deposition rates of approximately 60–

$90\text{ }\mu\text{m h}^{-1}$. During the film deposition on a single crystal, the film is strained owing to the mismatch between the film and the substrate. Thus, the mismatch affect the crystallinity, microstructure and electrical performance of YBCO films [12,13].

In the present study, we prepared YBCO films on SrTiO_3 (STO) by using laser CVD and investigated the effects of deposition temperature and lattice mismatch on the epitaxial growth, crystallinity, microstructure and critical temperature of the YBCO films.

2. Material and methods

The YBCO films were grown on a (100) STO single-crystal substrate ($10\text{ mm} \times 5\text{ mm} \times 0.5\text{ mm}$) using $\text{Y}(\text{DPM})_3$, $\text{Ba}(\text{DPM})_2/\text{Ba}(\text{TMOD})_2$ and $\text{Cu}(\text{DPM})_2$ (DPM; dipivaloyl-methanate and TMOD; 2,2,6,6-tetramethyl-3,5-octanedione) as precursors. The Ba precursor was a mixture of $\text{Ba}(\text{DPM})_2$ and $\text{Ba}(\text{TMOD})_2$ with a molar ratio of 4:1, which suppressed the decomposition of $\text{Ba}(\text{DPM})_2$ at temperatures greater than their eutectic point and vaporization at a constant rate.

*Corresponding author. Tel.: +81 22 215 2106; fax: +81 22 215 2107.

E-mail address: itonium@imr.tohoku.ac.jp (A. Ito).

The laser CVD apparatus was described elsewhere [10,11]. A continuous wave Nd:YAG laser (wavelength: 1064 nm) with laser power (P_L) from 0 to 200 W was used. The STO substrate was preheated on a hot stage at 873 K. The flow rates of the Ar and O₂ gases were 0.75 and 0.13 Pa m³ s⁻¹, respectively. The vaporization temperatures of the Y, Ba and Cu precursors were 440, 565 and 445 K, respectively. The composition of YBCO film analyzed by inductively coupled plasma spectrometry was Y:Ba:Cu = 1:2.1:3.6. The deposition temperature (T_{dep}) was measured with a thermocouple at the back side of the substrate. The total pressure was held at 0.6 kPa. The distance between the nozzle and the substrate was 30 mm. The deposition lasted 20 s. After deposition, the YBCO films were heat-treated at 573 K for 14.4 ks, 673 K for 14.4 ks and 773 K for 14.4 ks in pure O₂ atmosphere (100 kPa) to transform the orthorhombic structure of YBCO ($Pmmm$) to tetragonal structure ($P4_2m$).

The phase of the YBCO films was studied by X-ray diffractometer (XRD; Rigaku RAD-2C). The degree of the c -axis preferred orientation (f) of the YBCO films was calculated by using the Lotgering formula [14]:

$$f = \frac{P - P_0}{1 - P_0} \quad \text{where} \quad P = \frac{\sum I_{(00l)}}{\sum I_{(hkl)}} \quad \text{and} \quad P_0 = \frac{\sum I_{(00l)}^0}{\sum I_{(hkl)}^0}.$$

P represents the ratio of the sum of the XRD intensity of the c -axis-oriented YBCO peaks ($00l$) to the sum of the intensity of all the peaks (hkl) of the YBCO films from 10° to 60°. P_0 represents the corresponding ratio of the randomly oriented YBCO bulk (JCPDS #39-0486). The crystallinity of the YBCO films was evaluated by the full width at half maximum (FWHM) of the ω -scan (rocking curve) on the (200) or (005) reflection. The in-plane orientation of the YBCO films was measured by using a pole figure X-ray diffractometer (Rigaku Ultima IV). The schematic of the in-plane epitaxial growth relationship between the YBCO films and STO substrate was drawn by using VESTA [15]. The film microstructure was observed by using a field-emission scanning electron microscope (FESEM; JEOL JSM-7500F). The electrical resistivity was measured from 30 to 300 K by using the dc four-probe method. Au electrodes on the sample surface were prepared by an ion coater and connected to the resistivity measuring equipment with a thin copper wire (0.1 mm diameter).

3. Results and discussion

T_{dep} was increased from 928 to 1049 K by increasing P_L from 69 to 152 W. Fig. 1 shows the XRD patterns of the YBCO films prepared at T_{dep} = 947–1027 K. At T_{dep} < 928 K, no film was obtained. a -Axis-oriented YBCO films were prepared at T_{dep} = 928–947 K (Fig. 1(a)). YBCO films with a mixture of a -axis and c -axis orientations were prepared at T_{dep} = 968–988 K (Fig. 1(b)). c -Axis-oriented YBCO films were prepared at T_{dep} = 1006–1049 K (Fig. 1(c)). At

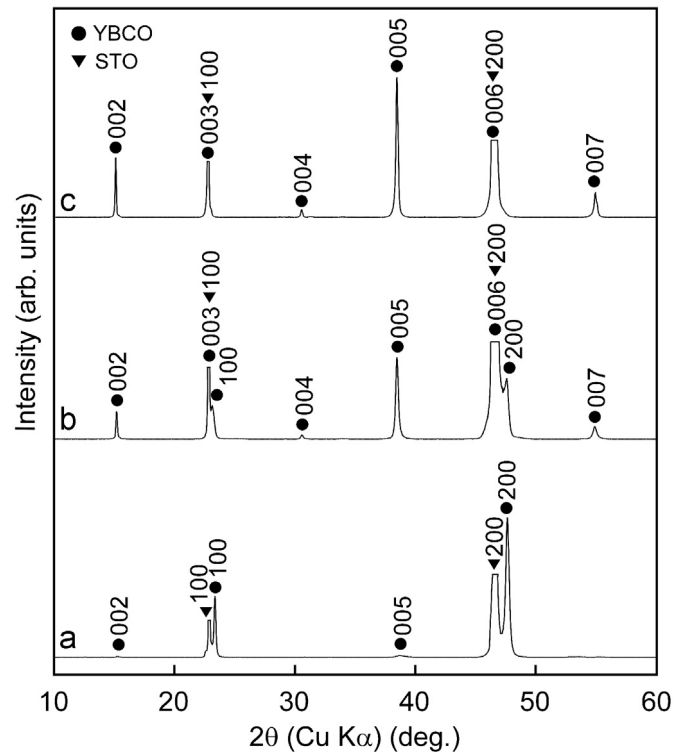


Fig. 1. XRD patterns of YBCO films prepared on (100) STO substrate at T_{dep} = 947 K (a), 968 K (b) and 1027 K (c).

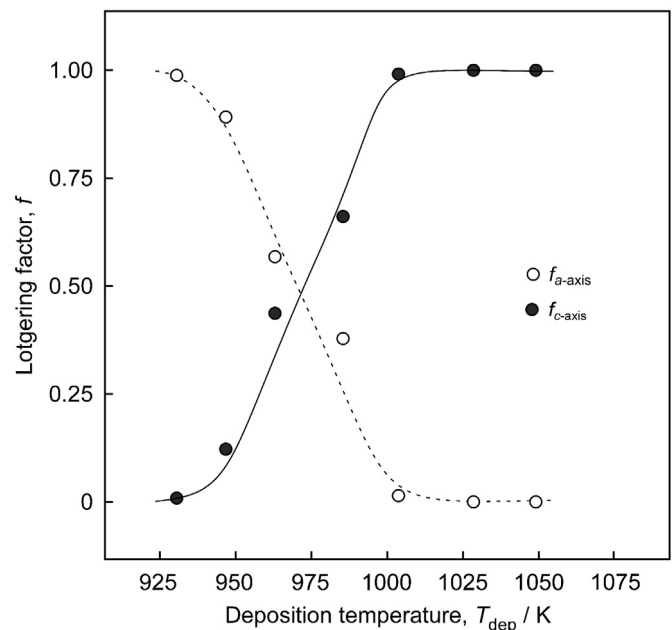


Fig. 2. a - and c -axis orientation of the YBCO films as a function of T_{dep} .

T_{dep} > 1049 K (P_L > 152 W), a small amount of Ba–Cu–O phase was present in the YBCO films. The degree of the preferred orientation (f) of the a -axis and c -axis is shown in Fig. 2. At T_{dep} = 928 K, f for the a -axis was 0.98 and that for c -axis was 0.02, indicating an almost fully a -axis-oriented YBCO film. With increasing T_{dep} , f for the c -axis

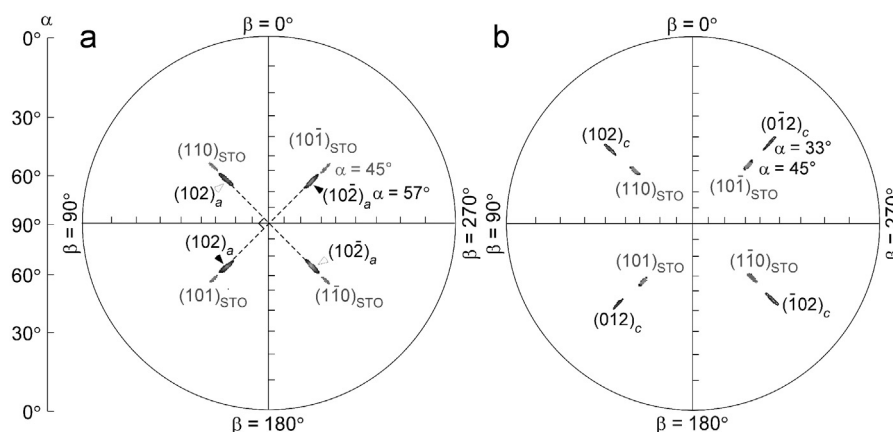


Fig. 3. X-ray pole figures of the (102) reflection in YBCO films grown on (100) STO substrate at $T_{\text{dep}}=947$ K (a) and 1027 K (b) and of the (110) reflection of the STO substrate.

increased and saturated to 1 at $T_{\text{dep}}=1006$ K, whereas f for the a -axis decreased and became 0 at $T_{\text{dep}}=1006$ K, suggesting fully c -axis-oriented YBCO films. The lower T_{dep} favoured the growth of a -axis-oriented grains, whereas the increase in T_{dep} favoured that of c -axis-oriented grains. For the laser CVD of YBCO films on MgO [10] and LAO [11], the dependence of T_{dep} on the preferred orientation is similar to that obtained in the present study.

Fig. 3 shows the X-ray pole figures of the (102) reflection of the YBCO films prepared at $T_{\text{dep}}=947$ –1027 K and those of the (110) reflection from the STO substrate. Their in-plane epitaxial relationships are also depicted in this figure. In the a -axis-oriented YBCO films, the pole figure of the YBCO (102) reflection exhibited a two-fold pattern at an elevation angle (α) of around 57° , which was attributed to the YBCO (102) and $(10\bar{2})$ planes with a complementary angle of 33° to the YBCO (100) plane. The four reflections with a repeating angle of 90° were due to the twinning structure or the multi-domain structure of the a -axis-oriented grains [16]. The azimuth angles (β) of the poles of the YBCO (102) reflection appeared at the same angles as the STO (110) reflection (Fig. 3(a)), suggesting the in-plane epitaxial relationship YBCO [001]//STO [001] and YBCO [100]//STO [100] for the a -axis-oriented YBCO grains.

In the c -axis-oriented YBCO films, the strong four-fold pattern originated from the c -axis-oriented YBCO grains and was attributed to the YBCO {102} planes with a complementary angle of 57° to the YBCO (001) plane (Fig. 3(b)). The angle β of the YBCO (102) reflections was at the same angle as the STO (110) reflections, thereby indicating the in-plane epitaxial relationship YBCO [100]//STO [010] and YBCO [001]//STO [100].

Fig. 4 shows the FWHM of the ω -scan and ϕ -scan of the YBCO films grown on STO substrate. In the a -axis-oriented YBCO films, the ω -scan on the (200) reflection was measured. The FWHM values of the ω - and ϕ -scans decreased from 0.8° to 0.6° with T_{dep} increasing from 928 to 968 K. The ω -scan on the (005) reflection was measured

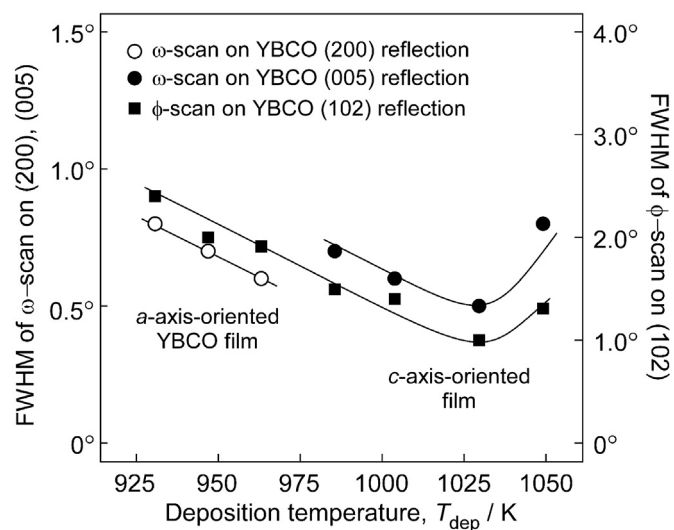


Fig. 4. FWHM of the ω -scan on the (200) and (005) reflections and of the ϕ -scan on the (102) reflection of the YBCO films on (100) STO substrate as a function of T_{dep} .

in the c -axis-oriented YBCO films. With T_{dep} increasing from 988 to 1049 K, the FWHM values of the ω - and ϕ -scans first decreased from 0.7° to 0.5° and then increased to 0.7° . A minimum of 0.5° corresponds to $T_{\text{dep}}=1027$ K. The ϕ -scan on the (102) reflection was measured in all YBCO films. The FWHM values first decreased from 2.4° to 1.0° and then increased to 1.3° with T_{dep} increasing from 928 to 1049 K, with the minimum of 1.0° at $T_{\text{dep}}=1027$ K.

Fig. 5 shows the surface and cross-sectional images of the YBCO films. At lower T_{dep} , i.e. 928–947 K, the a -axis-oriented YBCO films consisted of fine crystal grains of approximately 100 nm in size. With increasing the T_{dep} to 988 K, the microstructure of the a -axis- and c -axis-oriented YBCO films comprised needle-like grains and outgrowth particles distributed on a dense flat surface (Fig. 5(a, b)). The needle-like grains were a -axis-oriented YBCO grain, whereas the outgrowths were identified as Cu-rich particles [17–19]. The needle-like grains grew with orthogonal orientation on the film surface, which corresponded to

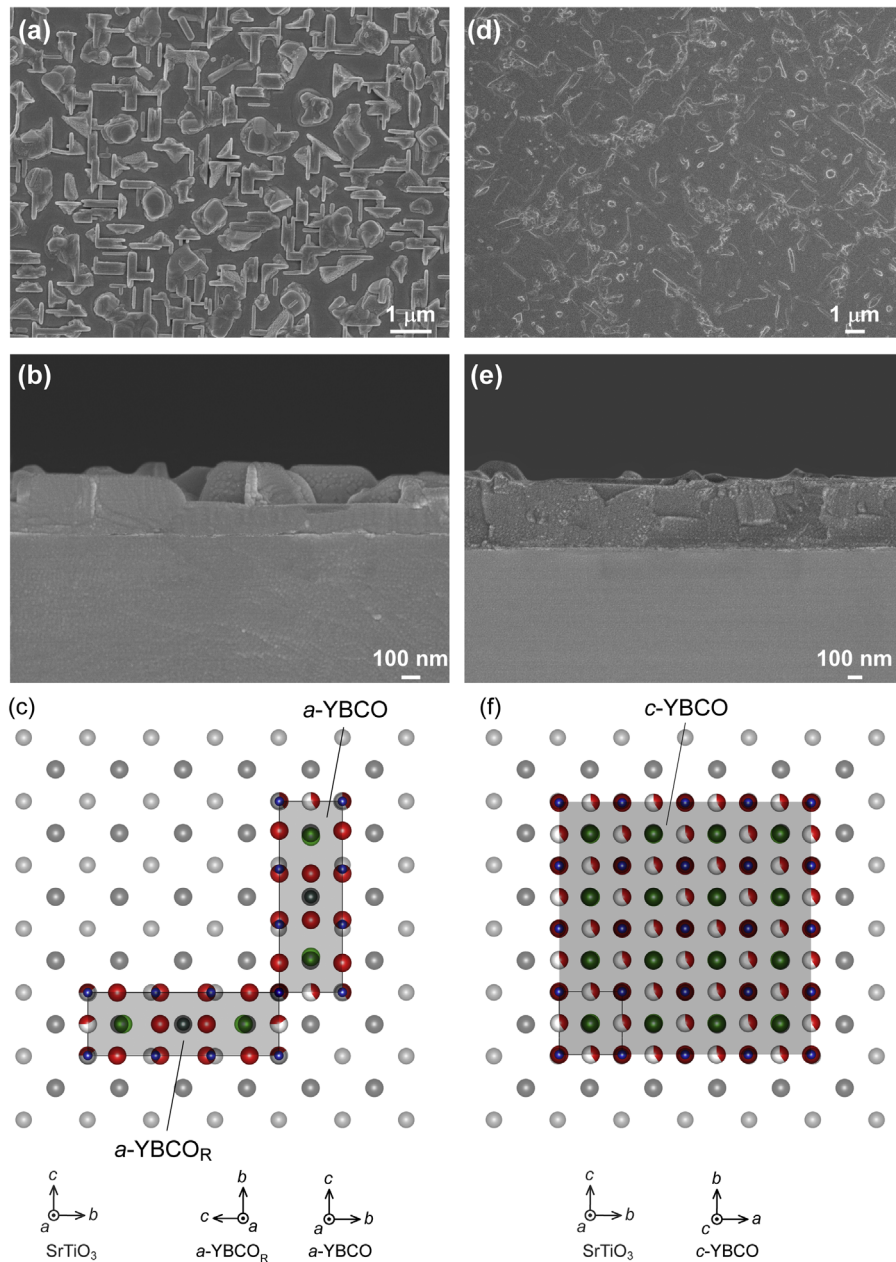


Fig. 5. Surface (a, d) and cross-sectional (b, e) SEM images of YBCO films grown at $T_{\text{dep}}=968$ K (a, b) and 1027 K (d, e). Images (c) and (f) depict the in-plane epitaxial relationships.

the multi-domain structure of *a*-axis oriented grains suggested by the pole figure (Fig. 3(a)) and derived the in-plane epitaxial growth model depicted in Fig. 5(c). As T_{dep} increased to 1006–1049 K, the *c*-axis-oriented YBCO films showed a dense surface and cross section (Fig. 5(d, e)). This was due to the excellent in-plane lattice matching between the *c*-axis oriented YBCO grain and (100) SrTiO_3 substrate (Fig. 5(f)). The amount of needle-like grains and outgrowth particles reduced significantly at high T_{dep} .

Fig. 6 shows the temperature dependence of the electrical resistivity of the YBCO films prepared at $T_{\text{dep}}=947$ K (*a*-axis-oriented YBCO film), 968 K (*a*-axis- and *c*-axis-oriented YBCO films) and 1027 K (*c*-axis-oriented YBCO

film). The electrical resistivity of the *a*-axis-oriented YBCO films showed semiconducting temperature dependence in the normal state and became zero at transition temperatures in the range of 30–50 K (Fig. 6(a)). The electrical resistivity of the *a*-axis- and *c*-axis-oriented YBCO films showed weak metallic temperature dependence above the superconducting transition and became zero at transition temperatures between 55 and 77 K (Fig. 6(a)). The resistivity of the *c*-axis-oriented YBCO films showed strong metallic temperature dependence in the normal state and sharp zero resistance transition at 78–90 K (Fig. 6(b)). Fig. 7 shows T_C versus T_{dep} of the YBCO films. T_C increased from 30 K at $T_{\text{dep}}=928$ to 90 K at $T_{\text{dep}}=1027$ K

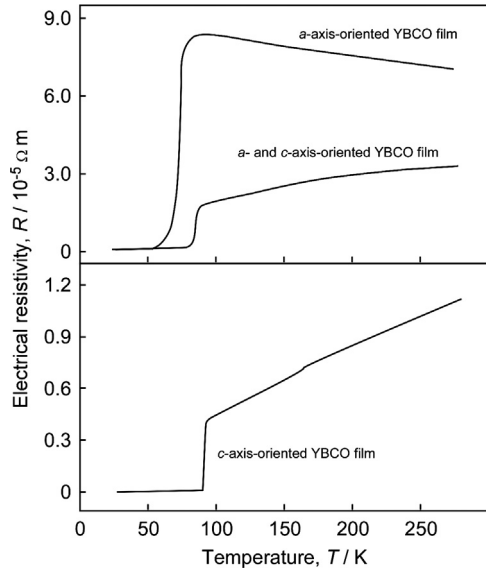


Fig. 6. Electrical resistivity as a function of the deposition temperature of the YBCO films grown on (100) STO substrate at $T_{\text{dep}}=947$ K (*a*-axis-oriented film), at 968 K (*a*- and *c*-axis-oriented film) and at 1027 K (*c*-axis-oriented film).

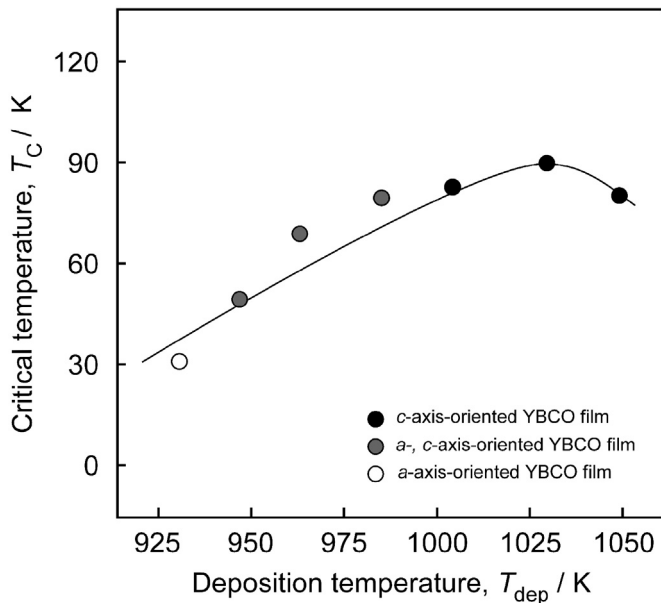


Fig. 7. T_C of the YBCO films grown on STO substrate as a function of T_{dep} .

and then decreased to 78 K at $T_{\text{dep}}=1049$ K. The highest T_C of 90 K was obtained at $T_{\text{dep}}=1027$ K. For the laser CVD YBCO films grown on MgO [10] and LAO [11], T_C as a function of T_{dep} exhibited similar tendencies to that reported in the present study, with the maximum T_C of 89 and 90 K.

Table 1 and Fig. 8 compare the FWHM of the ω -scan and ϕ -scan, T_C and the lattice mismatch of the YBCO films on the MgO [10], LAO [11] and STO substrates grown by laser CVD and MOCVD [20–23]. Our previous

Table 1

Comparison of the FWHM of the ω -scan, FWHM of the ϕ -scan, T_C and the lattice mismatch of YBCO films prepared on MgO, LAO and STO substrates by laser CVD and MOCVD.

| Method | Substrate | Orientation | ω -Scan (deg) | ϕ -Scan (deg) | T_C (K) | Mismatch (%) | Ref. |
|-----------|-----------|----------------|----------------------|--------------------|-----------|--------------|---------------|
| Laser CVD | MgO | <i>a</i> -Axis | 1.3 | 4.2 | 47 | 22.7 | 10 |
| | | <i>c</i> -Axis | 0.6 | 1.4 | 89 | 7.8 | |
| | LAO | <i>a</i> -Axis | 0.8 | 2.8 | 70 | 8.3 | 11 |
| | | <i>c</i> -Axis | 0.6 | 1.1 | 90 | 2.5 | |
| | STO | <i>a</i> -Axis | 0.7 | 1.9 | 67 | 0.9 | Present study |
| | | <i>c</i> -Axis | 0.5 | 1.0 | 90 | 0.5 | |
| MOCVD | MgO | <i>c</i> -Axis | 0.3–0.6 | – | 89 | 7.8 | 20, 21 |
| | LAO | <i>c</i> -Axis | 0.3 | 4.3 | 91 | 2.5 | 22 |
| | STO | <i>c</i> -Axis | 0.2–0.4 | – | 85–89 | 0.5 | 23 |

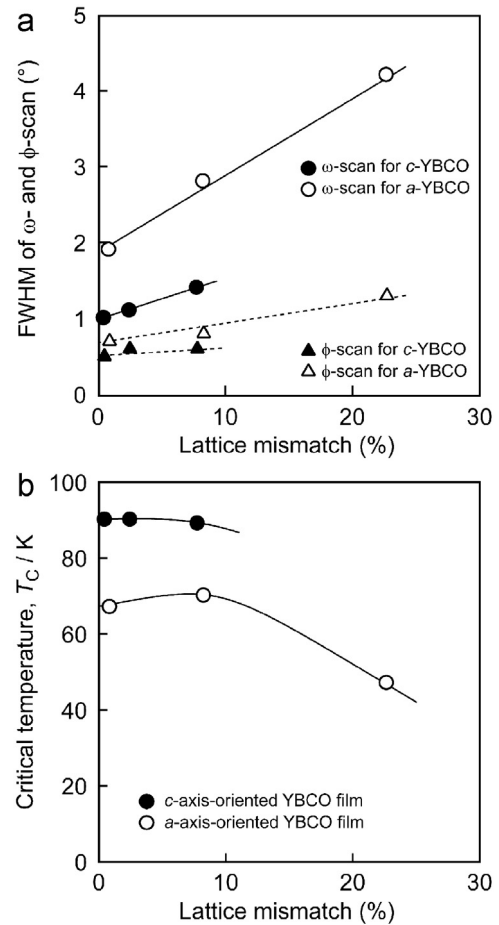


Fig. 8. Effect of lattice mismatch between YBCO films and substrates on the FWHM of ω -scan, ϕ -scan and T_C grown on MgO, LAO and STO substrates by laser CVD.

work showed that YBCO films grown on LAO substrate [11] have higher crystallinity and in-plane orientation than films grown on MgO substrate [10]. The reason is the lattice mismatch of 3.0% between LAO and YBCO that is

smaller than that of 8.6% between MgO and YBCO. On the other hand, the (100) STO single-crystal substrate and YBCO film have a lattice mismatch of 1.2%, which is smaller than that of (100) LAO (3.0%) and that of (100) MgO (8.6%). For the YBCO films on STO in the present study, the FWHM of the ω -scan showed smaller values of $0.5\text{--}0.7^\circ$ than that of $0.6\text{--}0.8^\circ$ on LAO [11] and $0.6\text{--}1.3^\circ$ on MgO [10]. The FWHM of the ϕ -scan of the YBCO films on STO showed a range of $1.0\text{--}1.9^\circ$ that is smaller than that of $1.1\text{--}2.8^\circ$ on LAO [11] and $1.4\text{--}4.2^\circ$ on MgO [10]. This was caused by the lattice mismatch of $0.5\text{--}0.9\%$ between YBCO and STO that is smaller than that of $2.5\text{--}8.3\%$ for LAO and of $7.8\text{--}22.7\%$ for MgO. In spite of the large lattice mismatch of $0.5\text{--}7.8\%$, the YBCO films have T_C close to zero. For the c -axis-oriented YBCO films grown on STO, LAO and MgO by laser CVD, T_C and the FWHM of the ω -scan and ϕ -scan were comparable to the films grown by MOCVD.

Fig. 9 shows the comparison of the R_{dep} of the YBCO films by MOCVD [24–33] and laser CVD [10,11,34]. For MOCVD, R_{dep} ranged from 0.01 to several micrometer per hour [24–33]. In the CVD process, high R_{dep} requires high T_{dep} and high precursor supply rate. However, the rate-limiting step of the CVD process changes from surface chemical reaction to gas phase diffusion at elevated T_{dep} and thus R_{dep} becomes saturated at high T_{dep} [30,33]. High supply rates increase R_{dep} [25,26,31,32], whereas, in the thermal CVD process, excess precursor supply causes a premature chemical reaction in the gas phase forming powder and an insufficient chemical reaction on the substrate that results in the depression of R_{dep} , the formation of a second phase and degraded orientation. On the other hand, for laser CVD, laser irradiation activates the chemical reaction not only on the substrate surface but also in the gas phase, giving rise to significantly high R_{dep} even under a

high precursor supply rate. The highest R_{dep} of the laser CVD YBCO films was up to $101\text{ }\mu\text{m h}^{-1}$, approximately 60–1000 times higher than that by MOCVD.

4. Conclusions

a -Axis- and c -axis-oriented YBCO films were grown on (100) STO single-crystal substrate by laser CVD. a -Axis-oriented YBCO films were prepared at $T_{\text{dep}}=928\text{--}968\text{ K}$ and c -axis-oriented films were prepared at $T_{\text{dep}}=988\text{--}1049\text{ K}$. For the c -axis-oriented YBCO films, the minimum FWHM of the ω -scan and ϕ -scan was 0.5° and 1.0° , respectively. The YBCO films on STO showed higher crystallinity, in-plane orientation and deposition rate than those on LAO and MgO. In addition, a high critical temperature of 90 K was observed in the c -axis-oriented YBCO films. The T_C and the FWHM of the ω -scan and ϕ -scan of the c -axis-oriented YBCO films grown by laser CVD were comparable to the films obtained by MOCVD even at a high-speed epitaxial growth ($58\text{--}101\text{ }\mu\text{m h}^{-1}$).

Acknowledgments

This work was supported in part by the International Superconductivity Technology Center (ISTEC). This work was also supported in part by the Japan Society for the Promotion of Science, and by MEXT, Japan, Grant-in-Aid for Scientific Research (A) (No. 22246082) and by the 111 Project, China (B13035).

References

- [1] H. Yamane, T. Hirai, K. Watanabe, N. Kobayashi, Y. Muto, Preparation of a high- J_c Y–Ba–Cu–O film at 700°C by thermal chemical vapor deposition, *Journal of Applied Physics* 69 (1991) 7948–7950.
- [2] J. Zhao, Y.Q. Li, C.S. Chern, P. Lux, P. Norris, B. Gallois, B. Kear, F. Cosandey, X.D. Wu, R.E. Muenchausen, S.M. Garrison, High-quality $\text{YBa}_2\text{Cu}_3\text{O}_{7-x}$ thin films by plasma-enhanced metalorganic chemical vapor deposition at low temperature, *Applied Physics Letters* 59 (1991) 1254–1256.
- [3] D. Berry, D.K. Gaskill, R.T. Holm, E.J. Cukauskas, R. Kaplan, R.L. Henry, Formation of high T_c superconducting films by organometallic chemical vapor deposition, *Applied Physics Letters* 52 (1988) 1743–1745.
- [4] V. Selvamanickam, Y. Xie, J. Reeves, Y. Chen, MOCVD-based YBCO-coated conductors, *MRS Bulletin* 29 (2004) 579–582.
- [5] J.K. Choi, B.H. Jun, C.J. Kim, Fabrication of YBCO coated conductors by MOCVD method using various templates, *Physica C* 445–448 (2006) 521–524.
- [6] T. Aytug, M. Paranthaman, L. Heatherly, Y. Zuev, Y. Zhang, K. Kim, A. Goyal, V.A. Maroni, Y. Chen, V. Selvamanickam, Deposition studies and coordinated characterization of MOCVD YBCO films on IBAD-MgO templates, *Superconductor Science and Technology* 22 (2009) 015008.
- [7] A. Molodyk, M. Novozhilov, S. Street, L. Castellani, A. Ignatiev, All-MOCVD technology for coated conductor fabrication, *IEEE Transactions on Applied Superconductivity* 21 (2011) 3175–3178.
- [8] A. Ito, H. Kadokura, T. Kimura, T. Goto, Texture and orientation characteristics of $\alpha\text{-Al}_2\text{O}_3$ films prepared by laser chemical vapor deposition using Nd:YAG laser, *Journal of Alloys and Compounds* 489 (2010) 469–474.

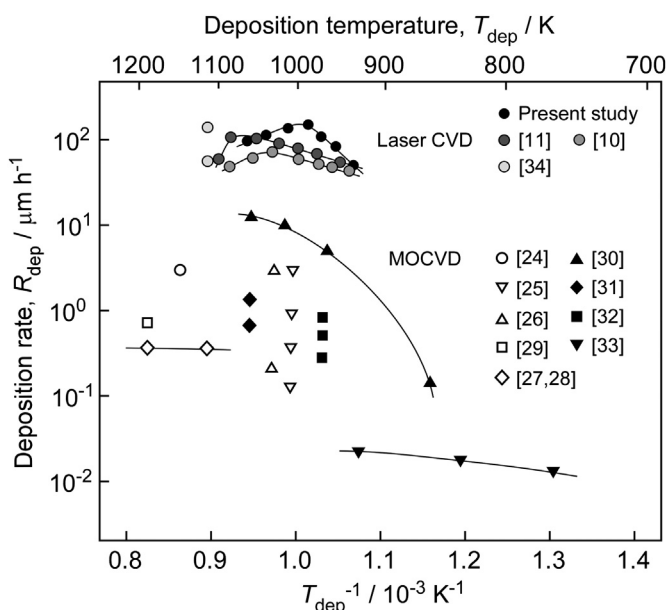


Fig. 9. R_{dep} of the YBCO films prepared by laser CVD and MOCVD.

- [9] D.Y. Guo, A. Ito, R. Tu, T. Goto, High-speed epitaxial growth of BaTi_2O_5 thick films and their in-plane orientations, *Applied Surface Science* 259 (2012) 178–185.
- [10] P. Zhao, A. Ito, R. Tu, T. Goto, High-speed growth of $\text{YBa}_2\text{Cu}_3\text{O}_{7-\delta}$ film with high critical temperature on MgO single crystal substrate by laser chemical vapor deposition, *Superconductor Science and Technology* 23 (2010) 125010.
- [11] P. Zhao, A. Ito, R. Tu, T. Goto, Fast epitaxial growth of a -axis- and c -axis-oriented $\text{YBa}_2\text{Cu}_3\text{O}_{7-\delta}$ films on (100) LaAlO_3 substrate by laser chemical vapor deposition, *Applied Surface Science* 257 (2010) 4317–4320.
- [12] J.P. Zheng, S.Y. Dong, H.S. Kwok, Texturing of epitaxial in situ Y-Ba-Cu-O thin films on crystalline substrates, *Applied Physics Letters* 58 (1991) 540–542.
- [13] K. Chiba, S. Makino, M. Mukaida, M. Kusunoki, S. Ohshima, The effect of lattice matching between buffer layer and $\text{YBa}_2\text{Cu}_3\text{O}_{7-\delta}$ thin film on in-plane alignment of c -axis oriented thin films, *IEEE Transactions on Applied Superconductivity* 11 (2001) 2734–2737.
- [14] F.K. Lotgering, Topotactical reactions with ferrimagnetic oxides having hexagonal crystal structures—I, *Journal of Inorganic and Nuclear Chemistry* 9 (1959) 113–123.
- [15] K. Momma, F. Izumi, VESTA 3 for three-dimensional visualization of crystal, volumetric and morphology data, *Journal of Applied Crystallography* 44 (2011) 1272–1276.
- [16] Y.L. He, G.C. Wang, A.J. Drehman, H.S. Jin, X-ray pole-figure analyses of $\text{YBa}_2\text{Cu}_3\text{O}_{7-x}$ thin film on $\text{SrTiO}_3(100)$ prepared by rf diode sputtering, *Journal of Applied Physics* 67 (1990) 7460–7466.
- [17] R. Ramesh, C.C. Chang, T.S. Ravi, D.M. Hwang, A. Inam, X.X. Xi, Q. Li, X.D. Wu, T. Venkatesan, Structural perfection of Y-Ba-Cu-O thin films controlled by the growth mechanism, *Applied Physics Letters* 57 (1990) 1064–1066.
- [18] T. Watanabe, N. Kashima, N. Suda, M. Mori, S. Nagaya, S. Miyata, A. Ibi, Y. Yamada, T. Izumi, Y. Shiohara, Rapid formation of 200 m-long YBCO coated conductor by multi-stage CVD, *IEEE Transactions on Applied Superconductivity* 17 (2007) 3386–3389.
- [19] N. Kashima, T. Watanabe, M. Mori, N. Suda, S. Nagaya, S. Miyata, A. Ibi, Y. Yamada, T. Izumi, Y. Shiohara, Developments of low cost coated conductors by multi-stage CVD process, *Physica C* 463–465 (2007) 488–492.
- [20] K.H. Young, D. Robinson, G.V. Negrete, T. Yamashita, T. Hirai, H. Suzuki, H. Kurosawa, L. Drabek, G. Grüner, Microstructure and microwave properties of YBCO thin films grown on MgO and SrTiO_3 by CVD, *Journal of Materials Research* 6 (1991) 2259–2263.
- [21] S. Aoki, T. Yamaguchi, N. Sadakata, O. Kohno, Characteristics of high T_c superconducting thin films prepared by chemical vapor deposition, *IEEE Transactions on Magnetics* 27 (1991) 1426–1429.
- [22] J.M. Zeng, P.C. Chou, X. Zhang, Z.J. Tang, A. Ignatiev, Single liquid precursor delivery photo-assisted metalorganic chemical vapor deposition of high quality $\text{YBa}_2\text{Cu}_3\text{O}_{7-x}$ thin/thick films, *Physica C* 377 (2002) 235–238.
- [23] T. Steinborn, G. Miehe, J. Wiesner, E. Brecht, H. Fuess, G. Wirth, B. Schulte, M. Speckmann, H. Adrian, M. Maul, K. Petersen, W. Blau, M. McConnel, Twinning of $\text{YBa}_2\text{Cu}_3\text{O}_7$ thin films on different substrates and modification by irradiation, *Physica C* 220 (1994) 219–226.
- [24] H. Yamane, H. Masumoto, T. Hirai, H. Iwasaki, K. Watanabe, N. Kobayashi, Y. Muto, Y-Ba-Cu-O superconducting films prepared on SrTiO_3 substrates by chemical vapor deposition, *Applied Physics Letters* 53 (1988) 1548–1550.
- [25] C.S. Chern, J. Zhao, Y.Q. Li, P. Norris, B. Kear, B. Gallois, Z. Kalman, Epitaxial thin films of $\text{YBa}_2\text{Cu}_3\text{O}_{7-x}$ on LaAlO_3 substrates deposited by plasma-enhanced metalorganic chemical vapor deposition, *Applied Physics Letters* 58 (1991) 185–187.
- [26] J. Zhao, Y.Q. Li, C.S. Chern, P. Norris, B. Gallois, B. Kear, B.W. Wessels, Superconducting $\text{YBa}_2\text{Cu}_3\text{O}_{7-x}$ thin films on silver substrates by in situ plasma-enhanced metalorganic chemical vapor deposition, *Applied Physics Letters* 58 (1991) 89–91.
- [27] Y.W. Ma, K. Watanabe, S. Awaji, M. Motokawa, New metalorganic chemical vapor deposition process in a high magnetic field for $\text{YBa}_2\text{Cu}_3\text{O}_7$, *Japanese Journal of Applied Physics* 39 (2000) L726–L729.
- [28] Y.W. Ma, K. Watanabe, S. Awaji, M. Motokawa, Evaporation of silver during chemical vapor deposition process for $\text{YBa}_2\text{Cu}_3\text{O}_7$ and its effect on microstructure, *Japanese Journal of Applied Physics* 40 (2001) 6339–6343.
- [29] H. Yamane, H. Kurosawa, H. Iwasaki, H. Masumoto, T. Hirai, N. Kobayashi, Y. Muto, T_c of c -axis-oriented Y-Ba-Cu-O films prepared by CVD, *Japanese Journal of Applied Physics* 27 (1988) L1275–L1276.
- [30] H. Abe, T. Tsuruoka, T. Nakamori, $\text{Y}_1\text{Ba}_2\text{Cu}_3\text{O}_{7-\delta}$ film formation by an OM-CVD Method, *Japanese Journal of Applied Physics* 27 (1988) L1473–L1475.
- [31] H. Yamane, H. Kurosawa, T. Hirai, Preparation of $\text{YBa}_2\text{Cu}_3\text{O}_{7-x}$ films by chemical vapor deposition, *Chemistry Letters* 6 (1988) 939–940.
- [32] K. Kanehori, N. Sughi, T. Fukazawa, K. Miyauchi, Low temperature growth of superconducting $\text{YBa}_2\text{Cu}_3\text{O}_{7-x}$ thin films by organometallic chemical vapour deposition, *Thin Solid Films* 182 (1989) 265–269.
- [33] S. Oda, H. Zama, S. Yamamoto, Superconductivity and surface morphology of YBCO thin films prepared by metalorganic chemical vapor deposition, *IEEE Transactions on Applied Superconductivity* 5 (1988) 1801–1804.
- [34] P. Zhao, A. Ito, R. Tu, T. Goto, High-speed preparation of c -axis-oriented $\text{YBa}_2\text{Cu}_3\text{O}_{7-\delta}$ film by laser chemical vapor deposition, *Materials Letters* 64 (2010) 102–104.